Molecular Biology of the Cell
Vol. 19, 2059–2068, May 2008

Rab8 Regulates Basolateral Secretory, But Not Recycling, Traffic at the Recycling Endosome

Lauren Henry and David R. Sheff

Department of Pharmacology, University of Iowa Carver College of Medicine, Iowa City, IA 52242

Submitted September 17, 2007; Revised February 5, 2008; Accepted February 11, 2008
Monitoring Editor: Jennifer Lippincott-Schwartz

Rab8 is a monomeric GTPase that regulates the delivery of newly synthesized proteins to the basolateral surface in polarized epithelial cells. Recent publications have demonstrated that basolateral proteins interacting with the μ1-B clathrin adapter subunit pass through the recycling endosome (RE) en route from the TGN to the plasma membrane. Because Rab8 interacts with these basolateral proteins, these findings raise the question of whether Rab8 acts before, at, or after the RE. We find that Rab8 overexpression during the formation of polarity in MDCK cells, disrupts polarization of the cell, explaining how Rab8 mutants can disrupt basolateral endocytic and secretory traffic. However, once cells are polarized, Rab8 mutants cause mis-sorting of newly synthesized basolateral proteins such as VSV-G to the apical surface, but do not cause mis-sorting of membrane proteins already at the cell surface or in the endocytic recycling pathway. Enzymatic ablation of the RE also prevents traffic from the TGN from reaching the RE and similarly results in mis-sorting of newly synthesized VSV-G. We conclude that Rab8 regulates biosynthetic traffic through REs to the plasma membrane, but not trafficking of endocytic cargo through the RE. The data are consistent with a model in which Rab8 functions in regulating the delivery of TGN-derived cargo to REs.

INTRODUCTION

The Rab proteins are small monomeric GTPases of the Ras family. More than 60 known Rabs collectively regulate the flow of nearly all membrane traffic within the cell (Pfeffer, 1994; Gurkan *et al.,* 2005; Jordens *et al.,* 2005). Of these, mammalian Rab8 has been associated with the flow of newly synthesized proteins to the basolateral surface in polarized epithelial cells (Huber *et al.,* 1993b; Moritz *et al.,* 2001). In yeast, the Rab8 homolog, sec4, is also required for the targeting of membrane traffic to the plasma membrane (Guo *et al.,* 1999). It has been suggested that Rab8 may be active in delivery of secretory cargo from the TGN to the plasma membrane. (Chen *et al.,* 1993; Huber *et al.,* 1993b). Studies of vesicular stomatitis virus protein G (VSV-G) delivery from the *trans*-Golgi network (TGN) have suggested that this process is regulated by Rab8, as dominant-negative (DN) mutants of Rab8 interfere with the delivery of basolateral cargo (Huber *et al.,* 1993b). Rab8 is not localized to the TGN; rather it is localized at or near the recycling endosome (RE) in both polarized and nonpolarized cells (Hattula *et al.,* 2006; Roland *et al.,* 2007). The function of Rab8 at the RE is likely to regulate recycling of membrane traffic, although its role in polarized sorting is not clear. Rab8 is not required for the delivery of all basolateral proteins, but appears to be obligatory in the case of those that bear a tyrosine-dependent basolateral-sorting determinant capable of interacting with the clathrin adapter μ1-B (Ang *et al.,* 2003). The basolateral TGN-to-plasma membrane trafficking pathway is not as direct as once thought. Recent reports demonstrate clearly that μ1-B–dependent basolateral traffic from the TGN passes through the RE en route to the plasma membrane (Ang *et al.,* 2004). This finding has prompted us to reevaluate the role of Rab8 in basolateral trafficking, in an effort to determine whether Rab8 controls passage from the TGN to the RE or from the RE to the plasma membrane.

In polarized kidney epithelia, such as Madin-Darby canine kidney (MDCK) cells, newly synthesized basolateral plasma membrane proteins are delivered "directly" to the basolateral plasma membrane without first passing through the apical membrane (Drubin and Nelson, 1996; Keller and Simons, 1997; Mostov *et al.,* 2000; Nelson, 2003; Hua *et al.,* 2006). With the notable exceptions of NgCAM, and polyimmunoglobulin receptor, apical proteins are likewise delivered to the apical plasma membrane without first being delivered to the basolateral surface (Breitfeld *et al.,* 1989, Anderson *et al.,* 2005; Hua *et al.,* 2006; Paladino *et al.,* 2006). Delivery to apical and basolateral domains is via separate transport vesicles (Wandinger-Ness *et al.,* 1990; Sztul *et al.,* 1991). This is in contrast to the situation in hepatocytes, where the majority of both the apical and basolateral proteins are first delivered basolaterally, after which the apical membrane proteins are endocytosed and sorted to the apical surface (Simons and Wandinger-Ness, 1990; Ihrke *et al.,* 1998). However, even direct delivery of nascent proteins to the basolateral surface implies only that these proteins are not first delivered to the apical surface; it does not preclude passage of these proteins through REs en route from the TGN to the basolateral surface. Thus, regulators of basolateral sorting, for example, Rab8 and the exocyst complex, could potentially act at the level of the TGN, the RE, the

This article was published online ahead of print in *MBC in Press* (http://www.molbiolcell.org/cgi/doi/10.1091/mbc.E07–09–0902) on February 20, 2008.

Address correspondence to: David R. Sheff (david-sheff@uiowa.edu).

Abbreviations used: CHO, Chinese Hamster ovary; MDCK, Madin-Darby canine kidney; MDCKT, MDCK cell with transferrin receptor; RE, recycling endosome; RFP, red fluorescent protein; TER, trans epithelial resistance; TGN, *trans*-Golgi network; Tfn, transferrin.

plasma membrane, or the pathways that link these organelles (Peranen *et al.*, 1996; Grindstaff *et al.*, 1998).

Sorting within the RE is a multistep process. Arriving ligands are first separated into distinct apical and basolateral subdomains within the RE, with ligands destined for each pathway thereby being concentrated (Thompson *et al.*, 2007). Apical and basolateral transport vesicles then bud from these ligand-enriched domains, a process that results in high fidelity of cargo sorting, at least along the basolateral transport pathway (Sheff *et al.*, 1999). Basolateral delivery of secretory proteins bearing tyrosine-based basolateral sorting determinants (such as transferrin receptor [TfnR], E-cadherin, and pIgR, as well as asialoglycoprotein receptor) involves sequential delivery from the TGN to the RE to the plasma membrane (Stoorvogel *et al.*, 1989; Futter *et al.*, 1995; Leitinger *et al.*, 1995; Ang *et al.*, 2004; Murray *et al.*, 2005; Cresawn *et al.*, 2007). Rab8 is known to regulate traffic along the TGN–RE–plasma membrane pathway, but whether this involves traffic into, through or out from the RE is not clear. Rab8 is also involved in AMPA recruitment to dendritic spines from the RE of neurons and thus may serve in both sorting and storage functions of the RE (Huber *et al.*, 1993a; Gerges *et al.*, 2004).

Given the diverse roles of Rab8 in a variety of contexts, it could potentially act 1) in the transport of vesicles from the TGN to the RE, perhaps controlling fusion into the RE; 2) in organizing the sorting of basolateral traffic into subdomains of the RE as vesicular traffic enters this structure; or 3) in budding from the RE and delivery of cargo to the plasma membrane, including the penetration of the actin-filament web near the plasma membrane(Peranen *et al.*, 1996; Hattula *et al.*, 2002). In an effort to resolve these issues, we examined the requirement for Rab8 in the polarized sorting of endocytic ligands and secreted proteins in MDCK cells. We find Rab8 to be associated with the basolateral secretion of proteins and the development of cell polarity. Surprisingly we find that Rab8 is not associated with endocytic recycling or basolateral delivery once cell polarity is established. Our results indicate that Rab8 is most likely involved in the TGN-to-RE transport step rather than in sorting at the RE or thereafter.

MATERIALS AND METHODS

Reagents

All chemicals used were of analytical grade or better and purchased from Sigma-Aldrich (St. Louis, MO) or Fisher Chemical (Fairlawn, NJ). Alexa-488 Tfn and Alexa-488 goat anti-mouse antibody were purchased from Molecular Probes (Invitrogen, Carlsbad, CA). Mouse monoclonal anti-gp114 was clone Y652, a gift from the Mellman laboratory.

Cell Lines and Constructs

MDCK cells stably expressing the human transferrin receptor (MDCKT) in pCB6 were previously described (Sheff *et al.*, 1999). DsRFP-Rab8 and dsRFP-Rab8 Q67L in adenoviral constructs and pShuttle-CMV as well as YFP-VSV-G tsO45 adenovirus construct were a kind gift from the Mellman laboratory. Adenovirus was produced in A-293 cells. Lentiviral constructs were made by first subcloning into the TA cloning vector pENTR/D Topo (Invitrogen) using a PCR product with primers CACCATGGCCTCCTCCGAGG and TCACAGAAGAACACATCGGAA. The red fluorescent protein (RFP)-Rab8 constructs were then transferred to pLenti4/V5 DEST using a clonase reaction according to manufacturer's directions (Invitrogen). Lentivirus was produced in F-293 cells with a Virapower support kit (Invitrogen) to supply packaging plasmids. Monoclonal antibodies against P58 and P114 were a kind gift from the Mellman laboratory.

Tfn Labeling and Kinetics

Tfn was labeled with ^{125}I using Iodo-Gen reagent (Pierce Chemical, Rockford, IL) as described (Podbilewicz and Mellman, 1990). MDCKT cells were grown to confluence on a 10-cm cell culture Petri dish. The cells were trypsinized and plated 1:1.1 into 24-mm Transwell filter inserts with 0.4-μm pore size (Corning Life Sciences, Corning, NY). For adenoviral and some lentiviral expressions, virus was applied 24 h after plating cells onto the filters. For day 3 lentiviral expression, the virus was applied 72 h after plating. All virus was applied in a minimal volume of unsupplemented DMEM media (Invitrogen/Invitrogen) for 1 h. Then growth media (DMEM with 8% fetal calf serum, pen/strep, and added glutamine) was substituted. All cells were induced with 5 mM butyrate overnight and then placed in butyrate-free medium for 4 h before analysis on day 4. Binding and recycling of Tfn as well as data handling, equations, and fitting of mathematical models was as described in detail previously (Sheff *et al.*, 1999, 2002). In particular, ^{125}I-labeled Tfn was selectively bound to the basolateral surface of the cells on ice for 45 min. After cells were washed on ice, the attached Tfn was chased into the cells with media containing 0.1 mg/ml unlabeled Tfn for up to 1 h. Internalization rates were derived from the clearance of acid-labile, labeled Tfn from the cell surface over 4 min. Recycling and transcytosis data were determined from counts released into the media at various times. These values were then used for further curve fitting of recycling data. k_{-1} is also derived from clearance values and indicates Tfn that is internalized and returns to the surface without passing through an acidic compartment, remaining bound to the receptor. Initial values for k_4 were derived from recycling rates at times <6 min (little contribution from the RE). Remaining values were calculated by iterative curve fitting, first by eye and then by minimizing the sum squared error (SSE) for each data set (Daniel, 1987). The SSE was derived using the following: $SSE = \Sigma$ ((average value of data at a given time point) $-$ (value predicted by model at the same time point))^2.

The SSE is useful for fitting a given model to a given data set by altering the values of the model variables (in this case the rate constants) because the better the fit, the smaller the SSE becomes. In this case a unique minimum SSE could be derived using each data set and each model. To determine whether a statistically significantly better fit was obtained by adding another parameter to the model (adding a value for k_6), we used the SSE derived for the best fit without k_6 and the SSE derived for the best fit of a model including a value for k_6 to derive the value of F, in Fischer's F test using the following formula: $F = (((SSE_1 - SSE_2)/(df_1 - df_2))/(SSE_2/df_2))$ (see Motulsky and Ransnas, 1987), where df represents the degrees of freedom (number of independent data points $-$ number of parameters fit by the model). Because F values vary with the number of degrees of freedom, a more useful comparison is to derive the probability p, that the additional parameter added to the model actually results in a better fit. For any given value of F and number of degrees of freedom df, a value p is obtained from a standard table (Daniel, 1987).

Endosomal Ablation

Recycling endosomes were specifically ablated using HRP-Tfn (Pierce Chemical) essentially as described in Ang *et al.* (2004). Briefly, MDCKT monolayers on Transwell filters (Corning Life Sciences) were labeled with horseradish peroxide (HRP)-Tfn, 0.010 mg/ml, in DMEM for 45 min at 37°C. The label was chased with label-free medium for 25 min. Cells were placed on ice and washed with PBS^{2+} (phosphate-buffered saline) three times. The filters were placed in PBS with 0.1 mg/ml 3,3′-diaminobenzidine (Sigma) with or without 0.025% H_2O_2. The reaction was stopped with PBS/bovine serum albumin (BSA; 1%, wt/vol).

VSV-G Labeling

YFP-VSV-G adenovirus was applied to MDCKT cells grown on Transwell filters 1 d after plating. Sixteen hours after infection, cells were shifted to 40°C and kept at that temperature until polarization and other manipulations were complete. To release the VSV-G, cells were moved to 31°C for 1 h, followed by 1 h at 37°C, followed by fixation.

Microscopy and Labeling

For localization of RFP-Rab8 in nonpolarized cells, Alexa-488 Tfn was bound to the cell surface on ice for 30 min and then chased into the cell at 37°C in the absence of further label for 25 min. Cells were fixed in 4% paraformaldehyde. For gp114 labeling, cells were first fixed and then permeabilized with 0.1% saponin in 2% BSA/PBS. Y652 antibody supernatant was applied at 1:100 with an Alexa 488 secondary label at 1:200. Images were acquired with a Zeiss Axiovert 200M microscope Jena Germany) equipped with a Hamamatsu (Hamamatsu, Japan) Orca ER cooled CCD camera and a 63× water immersion objective (Zeiss) using chroma filters optimized for fluorescein isothiocyanate (FITC) and rhodamine. For polarized MDCKT cells, labeling was from the basolateral surface only but otherwise as above. Images were acquired on a Zeiss LSM-50 confocal microscope with a Zeiss Axiovert 100M stand and a 63× oil immersion lens. Acquisition was in multitrack mode using excitation wavelengths of 488 and 543 with FITC and rhodamine filters. A stack of 30 images was taken over the cell height (typically 15 μm) with the raster zoomed to 2×. For three-dimensional (3D) reconstruction, the image stack was cropped to a single cell and then processed with Volocity (Improvision, Coventry, United Kingdom) software. An X-Z image was produced by cropping the image stack in the X-Y plane. X-Z images were produced using Zeiss LSM-510 software to acquire an X-Z image with 30 Z-sections.

RESULTS

To initiate our investigation of whether Rab8 acts on traffic passing from the Golgi to the RE versus on traffic passing from the RE to the plasma membrane, we first examined basolateral recycling of Tfn through the RE. MDCK cells stably expressing the human transferrin receptor (MDCKT) were grown in Transwell filter inserts and 24 h after seeding, were infected with an adenoviral construct expressing wild-type RFP-Rab8. This resulted in high expression levels in more than 85% of cells (as assessed visually, see Supplementary Figure 1). After an additional 3 d in culture during which the cells were allowed to complete their polarization, Tfn recycling was analyzed using ^{125}I-labeled Tfn (see *Materials and Methods*). Apical and basolateral media were collected at the indicated time points, and the total ^{125}I in each was measured (Figure 1A). In control cells, the recycled Tfn (released from the basolateral surface) represented 89.6 ± 3.3% of the total, whereas transcytosed Tfn (released from the apical surface) represented 6.1 ± 1.6%, an outcome that is consistent with previous studies (Sheff *et al.*, 1999, 2002). In contrast, when wild-type RFP-Rab8 was overexpressed, only 56.7 ± 2.7% of Tfn was recycled, whereas 39.0 ± 2.0% was transcytosed to the apical surface. These results suggested that overexpression of Rab8 as the cells were polarizing (and while at the time of the assay) led to mis-sorting of basolateral traffic in the endocytic system.

The kinetic data obtained from this initial experiment were used to theoretically analyze which of the pathways involved in endocytic recycling (shown in Figure 1B) is most likely perturbed. A mathematical model of traffic recycling through the endocytic system was fit to our Rab8 overexpression data, an approach we have used previously to localize endocytic trafficking defects that arise due to treatment with aluminum fluoride or latrunculin B (Sheff *et al.*, 1999, 2002). Using first-order rate constants for various endocytic trafficking pathways present in polarized cells (k_1–k_5, shown in Figure 1B), we were able to fit curves to the recycling data for both controls and cells overexpressing Rab8 (Figure 1C). The values derived from a best fit for all rate constants are shown in Table 1. Internalization rates (k_1) were determined directly as surface clearance over the first 4 min. The rate constant (k_1) for internalization of ^{125}I-Tfn was 0.853/min in control cells, whereas it was 0.488/min in RFP-Rab8–expressing cells (data not shown). This difference reflects a decrease in the rate of clearance from the cell surface after normalization for the number of receptors. There was also a difference in k_{-1}, which represents the rate of return to the plasma membrane for Tfn that has not encountered an acidic compartment (k_{-1}, 0.219 in control cells, 0.0 in infected cells). This discrepancy may be directly attributed to the lower internalization rate, which makes such traffic less likely. The values of k_1 and k_{-1}were then used to derive the remaining rate constants, by fitting the curves for the mathematical model to the recycling data (Table 1). Fitting of the model to experimental data were initially done by eye, after which the fit was fine-tuned by minimizing the SSEs for the fit of the model to each data set (see *Materials and Methods*). This best fit was made by iteratively altering values for all the rate constants involved, thus simultaneously exploring if changes in traffic between the plasma membrane and early and REs could explain the data. Multiple independent starting points were used for each curve fitting to ensure that a unique solution set with minimal SSE could be derived. Although there is no absolute SSE value for a good fit, a smaller SSE represents a better fit of the model to a given data set. The SSE for the fit of the model to control cells was 69.8. Surprisingly, the SSE for RFP-Rab8–overexpressing cells was 185.7. The large error in

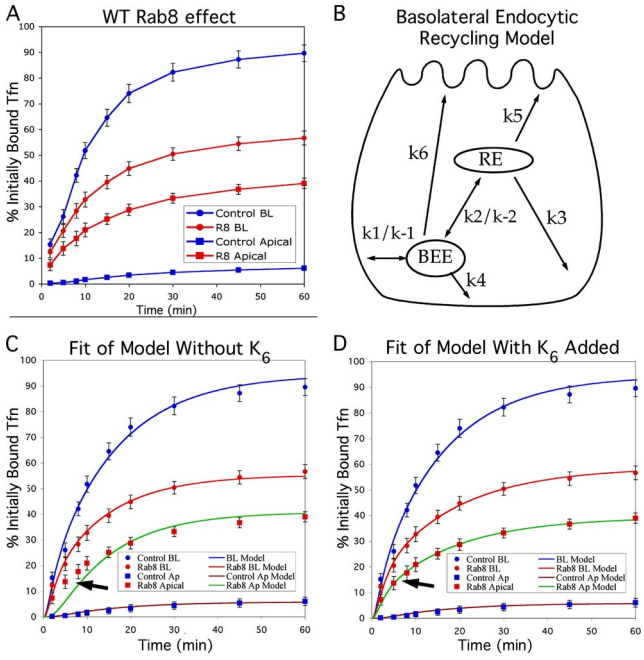

Figure 1. Rab8 overexpression before polarization causes mis-sorting of Tfn traffic by disrupting cell polarity. (A) Effect of Rab8 overexpression. ^{125}I-Tfn bound to the basolateral surface of MDCKT cells on ice was internalized at 37°C, and label released into the apical and basolateral media was measured at the times indicated. Blue circles, recycling into the basolateral medium in control cells; blue squares, transcytosis to the apical medium in control cells; red circles, recycling into the basolateral medium in cells overexpressing Rab8; and red squares, transcytosis into the apical medium in cells overexpressing Rab8. (B) Cartoon of possible Tfn recycling pathways, whose rate constants were used in the mathematical model. The rapid recycling pathway includes k_1 and k_4. The long recycling pathway includes k1 and k_3. k_6 indicates hypothetical mis-sorting pathway that would occur only in cells that are not properly polarized so that the apical and basolateral surfaces are functionally equivalent. BEE, basolateral early endosomes. (C) Fit of mathematical model to data in A using rate constants in Table 1, assuming $k_6 = 0$. Arrow indicates area of poor fit. Data points are as in A; blue line models recycling in control cells; brown line models transcytosis in control cells, red line models recycling in cells overexpressing Rab8; and green line models transcytosis in cells overexpressing Rab8. (D) Fit of mathematical model to data in A when loss of cell polarity is assumed. Data points and lines are as in C. Error bars, SD for experimental data. n = 9 for all data points.

Table 1. Values used for fit of kinetic model to Tfn recycling data

Rate constant	Control	Experimental without k_6	Experimental with k_6
k_1	0.853	0.488	0.488
k_{-1}	0.219	0	0
k_2	0.750	0.98	0.840
k_{-2}	0.001	0.009	0.001
k_3	0.061	0.034	0.033
k_4	0.215	0.23	0.249
k_5	0.005	.041	0.0236
k_6	0	0	0.145

Sum-squared error: 69.85, 185.7, and 21.2.

fit with respect to the data from the RFP-Rab8–overexpressing cells corresponded to a poor fit of the model to measurements of apical transcytosis at time points below 15 min (arrow in Figure 1C). Mathematical modeling allowed us to quantitatively compare a large number of possible Rab8 actions on the recycling pathways, for example, whether Rab8 resulted in a change in RE-to-plasma membrane traffic, to a change in early endosome to RE traffic, to both, or to neither. This allowed us to exclude changes in pathways k_1–k_5 as explanations for the effect of Rab8 on recycling traffic.

Normally, polarized cells contain separate apical and basolateral early endosomes that serve each surface domain (Bomsel *et al.*, 1989). However, cells that are improperly polarized allow the delivery of basolaterally internalized Tfn from the basolateral early endosomes to the apical surface, a pathway denoted as k_6 in Figure 1B (Sheff *et al.*, 2002). Addition of this pathway to the model for Rab8-infected cells resulted in a significantly better fit (arrow in Figure 1D shows area of improved fit), with an SSE of 21.3 (see Table 1; Daniel, 1987). To determine the statistical significance of this improvement, we used Fischer's F test (see *Materials and Methods*) In this case F = 61.7. Given the degrees of freedom available from our data set and including k_6 in our model, the probability is $p < 0.001$, that the added pathway (k_6) is statistically justified by the improvement in fit of the model to the experimental data. (Daniel, 1987; Motulsky and Ransnas, 1987). Other differences in the overall model included a diminishment of basolateral traffic from the RE (k_3, 0.061 in control cells vs. 0.033 in Rab8-overexpressing cells), and increased apical traffic from the RE (0.005 in control cells vs. 0.0236 in Rab8-overexpressing cells).

The kinetic results are consistent with Rab8 overexpression disrupting the apical-basolateral polarization of expressing cells, but could also represent a Rab8-infected monolayer that may not be intact. A leaky monolayer would give traffic recycled to the basolateral membrane direct access to the apical medium. Such a paracellular pathway would be topologically equivalent to k_6. To investigate the possibility that our results were due to monolayer leakiness, we applied ^{125}I-Tfn to the apical chamber of the Transwell system and measured leakage into the basolateral chamber at 4°C. Negligible leakage in monolayers of control cells, as well as in cells overexpressing RFP-Rab8 (0.09% for control cells, 0.1% for RFP-Rab8 expressing cells, and 10% for EDTA-treated cells), suggested that paracellular leakage was not abnormally high. To further test the integrity of the monolayer, we tested the transepithelial resistance (TER) at 37°C across the monolayer grown in a 12-mm transwell. Control cells had a specific TER of 104 Ù∗cm^2 (excluding the TER of the transwell membrane itself), and the RFP-Rab8–transfected cells had an almost identical TER of 95.3 Ù∗cm^2, again suggesting that paracellular leakage was not a factor in our results. Taken together, the results so far suggested that RFP-Rab8 overexpression during the time when cells would normally polarize leads to a profound disruption of apical-basolateral polarity in RFP-Rab8–expressing cells.

A defect in cell polarization could result from a disruption in the delivery of newly synthesized proteins, the recycling of polarized proteins, or both. Expression of RFP-Rab8 1 d after plating may disrupt the ability of cells to achieve apical-basolateral polarity as well as the ability of endosomes to maintain polarity if it is established. To differentiate between these possibilities, we sought to examine the effect of perturbing Rab8 both before polarization had occurred and afterward, in fully polarized cells. To this end, we used a lentivirus vector, which allowed for expression of Rab8 mutants in nondividing, fully polarized MDCKT monolayers. Although the lentiviral constructs were expressed in >90% of all cells (as judged by appearance of RFP in random fields examined by microscopy), protein expression per cell was less than that achieved with the adenoviral constructs used in the original experiments. In fact, expression levels of the wild-type Rab8 lentiviral construct were not sufficient to consistently alter Tfn traffic. We therefore utilized GTPase deficient (Q67L) DA Rab8 (DA-Rab8) and GDP-binding (T22N) DN RFP-Rab8 (DN-Rab8) constructs. These constructs are based on homology with the Ras GTPase. As previously described, the Q67L mutant binds GTP, whereas the T22N mutant does not (Peranen *et al.*, 1996). Both were expressed as lentiviral constructs. Rab proteins operate by cycling between GTP bound at the membrane and GDP bound in the cytosol. Therefore, although phenotypes of DA and DN mutants may vary, both would be expected to interfere with traffic along the regulated pathway, as evidenced by disruption of endoplasmic reticulum (ER)-to-Golgi traffic by the DA mutant of Sar1p GTPase (Oka and Nakano, 1994; Kimura *et al.*, 1995). When applied to MDCKT cells 24 h after plating (before the cells are polarized), the DA and the DN constructs each led to significant Tfn mis-sorting, although the mis-sorting at these expression levels (Figure 2, A and B) was not as great as that observed when wild-type Rab8 was expressed using adenovirus (Supplementary Figure 1). All Tfn recycling assays were performed

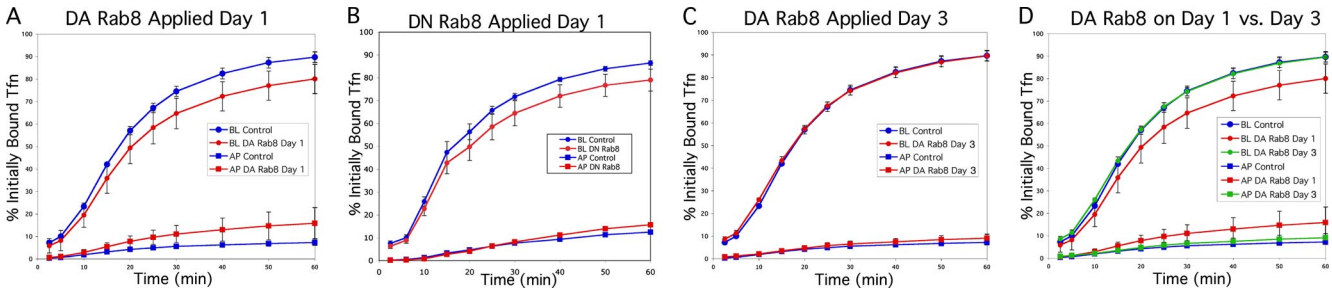

Figure 2. Dominant-active (DA) and -negative (DN) Rab8 mutants cause mis-sorting of Tfn traffic when applied before, but not after, cell polarity is established. All panels compare recycling (circles) and transcytosis (squares) of ^{125}I-Tfn in control cells (blue) and Rab8 overexpression mutants (red) after 4 d of polarization. (A) Lentiviral DA-Rab8 application 24 h after cell plating results in significant mis-sorting to the apical surface. (B) Lentiviral DN-Rab8 application 24 h after cell plating results in significant mis-sorting to the apical surface. (C) Lentiviral DA-Rab8 application 3 d after cell plating does not result in mis-sorting. (D) Overlay of results from control cells in A with those obtained for cells infected with DA-Rab8 in A and C, to directly compare the effects of infection after 24 h (red) versus 3 d (green).

4 d after plating, for consistency between assays and to ensure that all cells were polarized.

The DA-Rab8 construct was next applied to MDCKT monolayers 3 d after plating; this time point was chosen because the cells would be in the process of becoming polarized, but polarization would be completed before the construct was fully expressed (Thompson *et al.*, 2007). Consistent with the infection efficiency of this virus, >90% of the cells infected 3 d after plating expressed DA-Rab8 (as assessed by visual evaluation of RFP in cells in random microscope fields; Supplementary Figure 1). On the next day (4 d after plating), the expression level of DA-Rab8 was the same as that achieved in the previous experiment; however, Tfn traffic was not affected (Figure 2C). A direct comparison of cells infected with DA-Rab8 on days 1 and 3 (Figure 2D) illustrates the dramatic reduction of the Rab8 mutant effect after the cells have polarized. These results suggested that, although Rab8 is important for the establishment of cell polarity, it is not necessary for endocytic sorting and recycling of plasma membrane components. The possibility remained that even in polarized cells, Rab8 may affect secretory traffic passing from the Golgi to the RE (or to the plasma membrane), but not traffic arriving from the endocytic recycling pathway. These results, confirmed the kinetic analysis above, suggesting that the observed effects of wild-type Rab8 overexpression (when it occurs before polarization, i.e., 24 h after plating) on endocytic Tfn traffic were an indirect effect of a defect in cell polarization.

Because our results suggested that endocytic recycling traffic may not be directly affected by Rab8 activity, we wanted to confirm that our Rab8 constructs were correctly localized to the RE. Thus, wild-type RFP-Rab8 was expressed in MDCK cells using adenovirus (infected 24 h after plating). Tfn was bound to its receptors on ice and internalized for 25 min to specifically label the RE (Sheff *et al.*, 1999; Thompson *et al.*, 2007). Cells expressing relatively low levels of RFP-Rab8 were selected for visualization, and the RFP signal was found to colocalize with that of the internalized Alexa-488 Tfn (see X-Z reconstruction, Figure 3A). Similar results were obtained for DA-Rab8 expressed with lentivirus (data not shown).

We next visualized the distribution of the human Tfn receptor (TfnR) in the infected MDCKT cells. TfnR is normally distributed such that 93–95% of the receptor at the plasma membrane is at the basolateral surface, whereas 5–7% is present at the apical surface (Fuller and Simons, 1986; Sheff *et al.*, 1999). We used confocal microscopy to compare the localization of TfnR in cells infected with DA-RFP-Rab8 to that in uninfected cells. A lower multiplicity of infection (MOI) was used so that both infected and control cells would be present within a single field. Cells infected 24 h after plating were allowed to polarize before they were surface-labeled with Alexa-488 Tfn. In the control cells, Tfn labeling was confined to the basolateral surfaces (Figure 3, B and C, cells without red). In cells expressing DA-Rab8, however, apical labeling was observed, consistent with the presence of a defect in polarization (Figure 3B, arrows). In contrast, when the MDCKT cells were infected after polarization (3 d after plating), the distribution of TfnR was not disturbed by DA-Rab8 expression, nor was TfnR detectable at the apical surface (Figure 3C, arrows). These results suggested that TfnR polarity is sensitive to Rab8 disruption only before cell polarity is established.

Why would sensitivity to DA-Rab8 end with the establishment of cell polarity? It is possible that as the cell becomes polarized, redundant mechanisms ensure normal basolateral delivery, even in the presence of DA-Rab8. Alternatively, DA-Rab8 may affect the delivery of basolateral proteins from the secretory system, but not the recycling of basolateral proteins already at the plasma membrane, so that proteins mis-sorted during secretory delivery are resorted correctly during endocytic recycling. To differentiate between these possibilities, we used a construct in which YFP was fused with the temperature-sensitive VSV-G mutant, ts045. This mutant is trapped in the ER at the nonpermissive temperature of 40°C, but upon switching to the permissive temperature (31°C), a wave of the protein is released for processing through the Golgi. VSV-G was expressed in MDCKT cells using an adenoviral construct. Cells were infected 24 h after plating and were shifted to the nonpermissive temperature (40°C) 48 h after plating. Cells were allowed to polarize at the nonpermissive temperature until 4 d after plating, and then were shifted to 31°C for 1 h. Because it was possible that membrane trafficking may not proceed normally at this lower temperature, the cells were then shifted to 37°C for an additional 1 h. As is apparent from Figure 4 that the shift to 37°C did not result in sequestration of the VSV-G construct within the cell. We then tested the effect of DA-Rab8 expression by infecting the cells with DA-Rab8 (at 40°C) 3 d after plating. A low MOI was again used so that both control and DA-Rab8–expressing cells could be viewed in the same field. Further, we chose a time shortly after arrival of VSV-G at the cell surface so that there would not be time for correction of mis-sorted proteins through endocytic recycling and sorting. In this way, we could selectively observe VSV-G that had entered the secretory pathway after DA-Rab8 was expressed in cells that were fully polarized.

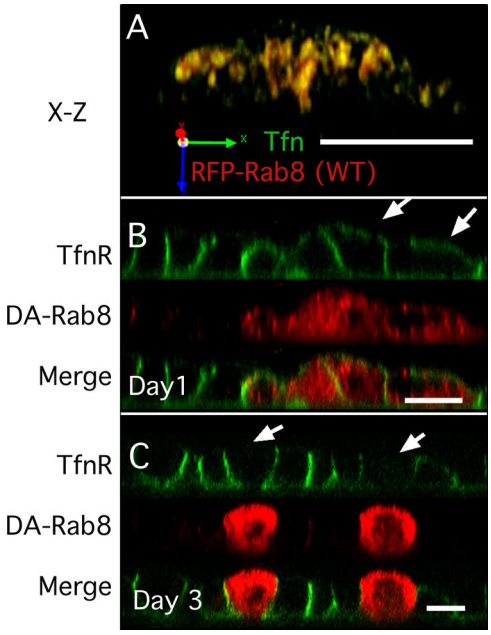

Figure 3. DA-Rab8 causes mis-sorting of TfnR when applied before, but not after, cell polarity is established. (A) X-Z reconstruction of an MDCKT monolayer infected with wild-type RFP-Rab8 (red) 24 h after plating and labeled with Alexa-488 Tfn internalized for 25 min (green, marks the RE). (B) X-Z reconstruction of MDCKT monolayer infected with DA-RFP-Rab8 (red) 24 h after plating and surface labeled on ice with Alexa-488 Tfn (green) on day 4. Arrows indicate mis-sorted TfnR. (C) MDCKT cells infected with DA-Rab8 (red) 3 d after plating and surface labeled on ice with Alexa-488 Tfn (green) on day 4 (green). Arrows indicate cells that express DA-Rab8 but did not mis-sort TfnR. Bar, 10 μm.

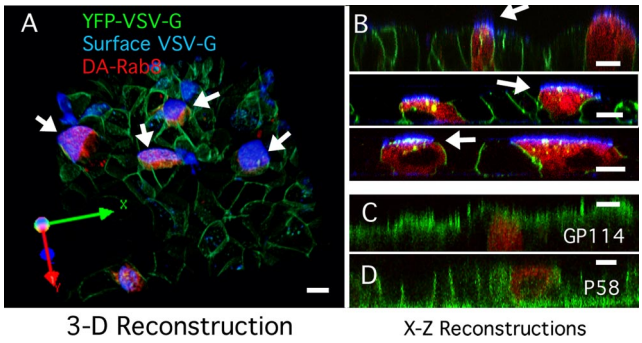

Figure 4. DA-Rab8 Rab8 applied 3 d after plating causes mis-sorting of VSV-G. (A) 3D reconstruction from a z-stack of confocal images spanning the full height of the cells. The image is rotated as shown by the axes at the lower left. GFP-VSV-G (green)–expressing MDCKT cells were infected with lentiviral DA-Rab8 at low MOI (red). Cells were kept at the nonpermissive temperature until 4 d after plating and then shifted to the permissive temperature as described in the text. The apical surface of live cells was labeled with an antibody against the VSV-G ectodomain (blue). All cells expressing DA-Rab8 (arrows) mis-sorted VSV-G to the apical surface. A few cells not expressing DA-Rab8 also mis-sorted VSV-G to the apical surface (top left) (B) Three X-Z reconstructions of confocal line-scan z-stacks from other fields of MDCKT cells labeled as in A, with arrows indicating mis-sorted VSV-G. (C) X-Z reconstruction of MDCKT cells expressing DA-Rab8 (red) as in A and labeled for apical marker GP114 (green). (D) X-Z reconstruction of MDCKT cells expressing DA-Rab8 (red) as in A and labeled for basolateral marker P58 (green). Bars, 10 μm.

We found that, in control cells >80% of VSV-G was delivered to the plasma membrane (Figure 4, A and B, cells with no red DA-Rab8), predominantly to basolateral areas and to a few puncta near the cell apex. To determine whether these puncta were external or internal, we also performed live-cell surface labeling, using an antibody that recognizes the VSV-G ectodomain. In control cells, some apical VSV-G staining was observed, (Figure 4A, blue in three cells in the top left of the field) but this was rare, involving ~8% of VSV-G–infected cells (assessed by counting affected cells in microscope fields). In contrast, 100% of the cells expressing DA-Rab8 (Figure 4, A and B, arrows) stained for VSV-G on their apical surfaces (Figure 4, A and B, blue). In X-Z cross sections, VSV-G was visualized at the apical surface of these cells (white arrows in Figure 4), as well as in internal puncta (Figure 4B, green/yellow puncta). These findings are consistent with mis-sorting of newly synthesized basolateral VSV-G to the apical surface in the presence of Rab8.

The introduction of Rab8 3 d after plating caused mis-sorting of newly synthesized VSV-G, but this may also have reflected a general loss of apical-basolateral polarity in the treated cells. Although this seemed unlikely because endosomal recycling was unaffected under these conditions, we confirmed that the cells were polarized by staining for the endogenous proteins GP114 and P58. Because both of these proteins are made constitutively and have long half-lives, the bulk of the protein should have been delivered and polarized before DA-Rab8 was introduced. Further, we expected that defects in polarization would be corrected gradually, through the normal endocytic sorting process. GP114 is a marker for the apical plasma membrane and has been reported to be delivered normally in the presence of Rab8 mutants. We confirmed this observation here (Figure 4C). P58 is the beta subunit of the Na^+/K^+ ATPase and is normally expressed basolaterally. Like the TfnR (Figure 3), P58 was normally distributed in cells expressing DA-Rab8. Taken together with the results above, these findings suggested that DA-Rab8 expression selectively disrupts the delivery of newly synthesized basolateral proteins without affecting established cell polarity or the fidelity of endocytic sorting.

Basolaterally targeted VSV-G traffic is reported to pass through the RE. Our results suggested that DA-Rab8 disrupts secretory traffic without affecting the recycling pathway. This could result from either a disruption of TGN-to-RE traffic or a bypass of the RE by direct TGN-to-plasma membrane traffic. To determine if traffic disruption at the RE could be responsible for these results, we took an organelle-ablation approach, using Tfn-HRP to ablate the RE (Hopkins, 1983; Stoorvogel *et al.*, 1988; Pond and Watts, 1997). This approach was previously used in glass-grown (incompletely polarized) MDCK cells to ablate the RE, which resulted in trapping of VSV-G secretory traffic at the Golgi (Ang *et al.*, 2004). The method has also been used to ablate REs in fully polarized MDCK cells, although in the latter case apical mis-sorting of VSV-G was not directly examined (Ang *et al.*, 2004; Cresawn *et al.*, 2007). In the current study, MDCKT monolayers were incubated with Tfn-HRP conjugate for 45 min, followed by a chase with serum-free medium for 25 min to allow the RE to be targeted this is a longer chase period than used by Ang *et al.* (2004). The cells were then treated with diaminobenzidine (DAB) and H_2O_2 for 1 h on ice, to allow for the formation of an insoluble precipitate in the HRP-containing compartment. This results in the effective ablation of the RE, and importantly, prevention of all trafficking to and from the affected structure. To ensure that only the RE was ablated, we internalized Alexa 546-Tfn for 8 min (Figure 5A) and checked for the usual labeling of early endosomes and REs. Although REs as well as early endosomes were clearly visible in control cells (Figure 5, A and B, large arrows, no H_2O_2), only peripheral small endosomes could be discerned in cells that had undergone the full ablation treatment (Figure 5A, small arrows). We define early endosomes and REs functionally so that early endosomes are those that contain Tfn internalized for 2.5 min, whereas REs contain Tfn internalized for 25 min. To further confirm that the perinuclear REs had been ablated, we used a double-labeling protocol, internalizing Alexa 488-Tfn for 25 min and Alexa 546-Tfn for 2.5 min in the same cells. This allowed visualization of functional early endosomes and REs. Perinuclear REs were clearly visible in control cells (Figure 5C, green), but were absent in the cells that had undergone the ablation treatment (Figure 5D; note absence of green). Early endosomes were visualized by Tfn internalized for 2.5 min in both control and ablated cells (Figure 5, B and C, red), indicating that early endosomes were still present and functional. Because Alexa 488-Tfn was no longer visible in the ablated cells, it must have recycled out of the cells. Such rapid recycling would be consistent with direct recycling from the early endosomes to the plasma membrane (pathway k_4 in Figure 1B) rather than through the RE (pathways k_2 and k_3 in Figure 1B).

To determine if cell polarity was acutely disrupted by the ablation technique, we again visualized the endogenous proteins GP-114 and P58. GP114 was apically localized in both the control and RE-ablated cells (Figure 5, E and F). Similarly, P58 was basolaterally localized in both control and RE-ablated cells (Figure 5, G and H). These results suggested that ablation of the RE did not acutely disrupt preformed cell polarity, consistent with our observations for DA-Rab8.

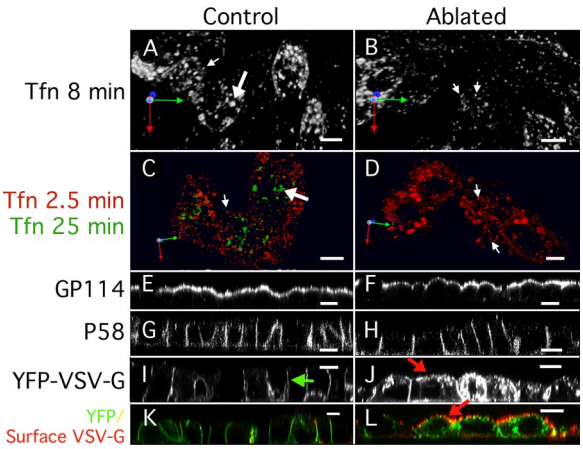

Figure 5. Ablation of the RE causes mis-sorting of newly synthesized VSV-G. All panels show MDCKT cells (4 d after plating) that have internalized Tfn-HRP into the RE. (A, C, E, G, I, and K) Control cells treated with DAB but not H_2O_2; (B, D, F, H, J, and L) cells treated with DAB and H_2O_2. (A and B) Basolaterally applied Alexa-546 Tfn internalized into MDCKT cells for 8 min labels early (small arrow) and recycling (large arrow) endosomes. REs are not visible in RE-ablated cells. (C and D) Basolaterally applied Alexa-546 Tfn internalized into control MDCKT cells for 25 min labels RE (large arrows). Small peripheral early endosomes are visible in RE-ablated cells (small arrows). (E and F) In MDCKT cells labeled for Gp-114, both control and RE-ablated cells are labeled apically. (G and H) In MDCKT cells labeled for p58, both control and RE-ablated cells are labeled basolaterally. (I and J) MDCKT cells expressing VSV-G tsO45 released at the permissive temperature for 2 h after RE ablation. Green arrow in I indicates normal basolateral distribution of VSV-G. Red arrow in J indicates putative apical VSV-G in RE-ablated cells. (K and L) MDCKT cells as in I and J containing cellular GFP-VSV-G (green) and with surface VSV-G labeled by anti-VSV-G ectodomain antibody (red). Red arrow indicates mis-sorted apical VSV-G in ablated cells. Bars, 10 μm.

To determine if polarized delivery of newly synthesized proteins was affected by RE ablation, we again used VSV-G. Tfn-HRP was internalized, at the nonpermissive temperature, in MDCKT cells expressing VSV-G. After ablation, the cells were shifted to 31°C for 1 h and then to 37°C for 1 h. In control cells, VSV-G was delivered to the basolateral surface (Figure 5I, green arrow), but in cells that had undergone ablation treatment, VSV-G was observed in many intracellular structures. In the ablated cells, some of the VSV-G appeared to be at or near the apical surface (Figure 5J, red arrow). To determine if the VSV-G had been delivered to the apical surface, live cells were labeled with an antibody directed against the VSV-G ectodomain, as had been done for DA-Rab8–expressing cells. Little or no surface labeling for VSV-G was observed in control cells (Figure 5K), but at least some apical VSV-G signal was visible in virtually all of the ablated cells (Figure 5L, red arrow). These results suggested that, when the RE is not available to receive newly synthesized traffic from the TGN, at least some of that traffic is rerouted to the apical plasma membrane. Together these results suggest that both HRP-mediated ablation of the RE and the expression of DA-Rab8 both lead to the diversion of secretory traffic to the apical plasma membrane at the RE.

DISCUSSION

Because its discovery, Rab8 has been associated with the regulation of basolateral traffic in polarized cells. However, rather than being localized to the plasma membrane, Rab8 is present in the peri-Golgi area, which includes the Golgi, TGN, and RE. It is now clear that basolateral cargo from the TGN—including the TfnR, VSV-G, asialoglycoprotein receptor, pIgR, and e-cadherin—passes through the RE. Our observations and those of others are consistent in that Rab8 appears to be associated with the RE rather than the Golgi. In contrast to basolateral traffic, apical traffic is Rab8-independent and does not appear to pass through the RE, but rather through other apical endosomal organelles. Together, these findings suggest that basolateral delivery is a two-step process that involves sorting at the TGN, along with what may be a secondary, or quality-control, level of sorting at the RE (Figure 6). Our findings are consistent with Rab8 controlling the delivery of basolateral secretory traffic from the TGN to the RE, rather than functioning later in the process of delivery to the surface.

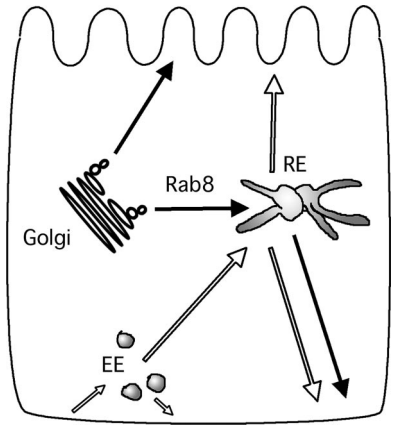

Figure 6. Cartoon of trafficking pathways that pass through the RE. Solid arrows represent secretory pathways. Open arrows represent recycling pathways. EE, early endosome; RE, recycling endosome.

Rab8 Does Not Regulate Basolateral Endocytic Traffic Directly

Given that Rab8 is associated with the RE, it could be involved in trafficking to the RE, sorting within the RE, or trafficking out of the RE. The most direct way to examine both sorting within the RE and basolateral traffic out of the RE was to monitor endocytic recycling of Tfn through the RE (Figure 6). We found that the overexpression of wild-type Rab8 and the introduction of Rab8 mutants before cell polarity was established had substantial effects on endocytic traffic, whereas the introduction of DA-Rab8 after the cells were polarized did not disrupt endocytic traffic. This latter finding was surprising in light of the fact that Rab8 had previously been reported to be important for basolateral delivery in general.

We sought to resolve why Rab8 mutants had an effect on basolateral traffic when introduced before polarization, but not after polarization. To this end we used a kinetic analysis of the trafficking that was induced by Rab8 overexpression before polarization. This analysis allowed us to test a large number of hypothetical variations in trafficking against the experimental data, using a quantitative mathematical model. Quantification allowed us to examine changes in trafficking not only into or out of the RE, but also along any of the other known recycling pathways, alone or in combination, and then test which solution set of hypothetical changes fit most closely to the experimental data. We started

with data sets of wild-type Rab8 overexpression (Rab8 expressed 24 h after plating), which showed clear disruption in the polarized delivery of endocytosed Tfn. Contrary to our initial expectations, we did not find a significant disruption of trafficking at the RE, or even a combination of disruptions along normal trafficking pathways, that could explain the overall loss of polarized sorting in the endocytic pathway. Rather, a model in which Rab8 overexpression disrupted the apical-basolateral polarization of the affected cells was most consistent with the data. This depolarization resulted in aberrant delivery, with the cargo of basolateral early endosomes being mis-routed to the apical surface. Immunofluorescence examination of DA-Rab8–expressing cells in an otherwise normal MDCKT monolayer confirmed that these cells were not normally polarized when the DA-Rab8 was introduced before cell polarization was complete. Together these results lead us to conclude that Rab8 did not directly regulate endocytic recycling in individual endocytic compartments, but rather, it did disrupt the establishment of cell polarity. In this way, cargo from the basolateral early endosomes is no longer restricted to either basolateral recycling or delivery to the RE. Instead, this basolateral cargo can be delivered directly to the apical surface of the poorly polarized cell. This is consistent with Rab8 functioning in the secretory pathway but not in the endocytic, pathway. Because the secretory and endocytic pathways to overlap after passing through the RE (Figure 6), these results would suggest that Rab8 acts on secretory traffic in transit from the TGN to the RE.

Rab8 Regulates Biosynthetic Basolateral Traffic Both Before and after Cell Polarize

One alternative to this conclusion, is that Rab8 function shifts as the cells polarize. Perhaps Rab8 controls a direct TGN to plasma membrane pathway in cells before they achieve polarity, but this becomes less important afterward. A similar suggestion has been made for the clathrin adapter μ1-B, which is required for biosynthetic and recycling basolateral delivery of TfnR before cells are polarized, but not for biosynthetic delivery after polarization (Gravotta *et al.*, 2007). We therefore tested whether DA-Rab8 had an effect on biosynthetic delivery, when introduced 3 d after plating the cells. Under these conditions, changes in endocytic function were not detected. Using a pulse of temperature-sensitive GFP-VSV-G, we were able to detect VSV-G mis-sorting when DA-Rab8 was introduced after polarization. The pulse was after expression of DA-Rab8 and was sufficiently short that endocytic resorting of VSV-G to the correct plasma membrane domain could not have occurred. This finding supports a model in which Rab8 continues to be required for the basolateral delivery of newly synthesized proteins even in polarized cells. The fact that endogenous basolateral as well as apical markers were normally distributed may be explained by their relatively long half lives, so that normal sorting and delivery occurred before DA-Rab8 was expressed. Additionally, as these proteins were in the cell for many hours, there would be endocytic resorting of any mis-directed protein, not affected by DA-Rab8.

Rab8 Acts on the TGN-to-RE Pathway Not on a Separate TGN-to-Plasma Membrane Pathway

Much of our interpretation relies upon the assumption that most, or all, of the basolateral biosynthetic traffic passes through the RE. This assumption is supported by both old and recent observations. It is well established that the trafficking of newly synthesized and recycling basolateral membrane proteins relies upon the same set of basolateral targeting determinants (Matter *et al.*, 1993). Recently, a study using a slowed-down transport system and HRP ablation of the RE in glass-grown MDCK cells has taken this understanding further, showing the RE to be an intermediate in the basolateral secretory pathway. Ablation of the RE using HRP resulted in the intracellular trapping of VSV-G in the majority of cells, although some cells did express VSV-G on their surfaces (Ang *et al.*, 2004). Because the cells were not fully polarized, it is difficult to interpret whether this represented mis-sorting or a bypass of the ablated RE. Further analysis of basolateral and apical trafficking in fully polarized, filter-grown MDCK cells also found passage through the RE to be an essential step in the delivery of VSV-G to the basolateral surface in fully polarized MDCK cells (Cresawn *et al.*, 2007).

In blocking delivery of basolateral secretory traffic to the RE, we observed mis-sorting to the apical surface. This finding differs somewhat from those published by both Ang and Cresawn (Ang *et al.*, 2004; Cresawn *et al.*, 2007). These discrepancies may be attributable, in part, to the fact that we used fully polarized MDCK monolayers and used Ab detection of apically mis-sorted VSV-G rather than YFP detection alone. Additionally, we used a longer (25 min) chase period to ensure that REs were ablated. Both recycling through early endosomes and the Golgi morphology (data not shown) were unaffected by this procedure. Under these conditions, normal cell polarity was maintained, but newly synthesized VSV-G was mis-sorted to the apical surface. Others have demonstrated that the apical pathway does not pass through the RE. The findings presented here establish that when the RE is not available to receive traffic, mis-sorting from the TGN to the apical surface occurs. This traffic may also pass through an endocytic compartment serving the apical surface only. Such would also appear to be the case when Rab8 mutants are used to disrupt TGN-to-RE traffic.

CONCLUSIONS

On the basis of our assessments of morphology, endocytic recycling traffic, and secretory traffic, we would suggest a model of the system in which Rab8 regulates traffic from the TGN to the RE along the TGN–RE–plasma membrane route. This interpretation implies that basolateral trafficking out of the RE and fusion at the plasma membrane are not Rab8 dependent. Thus, one potential role for Rab8 might be to mediate fusion events between transport vesicles generated at the TGN and the RE. Although we favor this interpretation, another possible interpretation is that TGN traffic through the RE is directed to a unique subdomain of the RE that exits in a Rab8-dependent manner. If this is the case, then Tfn-HRP ablation would fill the organelle and thus disrupt TGN–RE–plasma membrane traffic, whereas exit of Tfn and Rab8 dependent secretory traffic from the RE to the plasma membrane would be along separate pathways. Differentiation between these possibilities will have to await further analysis. It is thus not inconceivable that Rab8 may accompany a variety of cargoes out of the TGN, even to differing targets (Deretic *et al.*, 1995; Moritz *et al.*, 2001). For example, in addition to basolateral traffic, Rab8 has been implicated in TGN-to-primary cilium traffic (Nachury *et al.*, 2007). Rab8 is dispersed in cells from patients with the ciliopathies autosomal dominant polycystic kidney disease and Bardet-Biedel syndrome (Charron *et al.*, 2000; Nachury *et al.*, 2007). The primary cilium appears to be a domain separate from either apical or basolateral plasma membrane domains, which shares some characteristics with the basolateral domain (Rogers *et al.*, 2004). It is possible that Rab8-mediated

secretory traffic to the primary cilium also passes through an endocytic compartment or may even be sorted from basolateral traffic not at the TGN, but later in the RE. These possibilities will require further investigation.

ACKNOWLEDGMENTS

We are especially indebted to Agnes Ang, and Ira Mellman (both of Genentech) for providing the dsRFP-Rab8 constructs as well as the YFP-VSV-G tsO45 mutant construct. We also thank Heike Folsch and Bettina Winkler for consultation and advice. This work was supported in part by a grant to D.S. from the American Heart Association (0335078N).

REFERENCES

Anderson, E., Maday, S., Sfakianos, J., Hull, M., Winckler, B., Sheff, D., Folsch, H., and Mellman, I. (2005). Transcytosis of NgCAM in epithelial cells reflects differential signal recognition on the endocytic and secretory pathways. J. Cell Biol. *170*, 595–605.

Ang, A. L., Folsch, H., Koivisto, U. M., Pypaert, M., and Mellman, I. (2003). The Rab8 GTPase selectively regulates AP-1B-dependent basolateral transport in polarized Madin-Darby canine kidney cells. J. Cell Biol. *163*, 339–350.

Ang, A. L., Taguchi, T., Francis, S., Folsch, H., Murrells, L. J., Pypaert, M., Warren, G., and Mellman, I. (2004). Recycling endosomes can serve as intermediates during transport from the Golgi to the plasma membrane of MDCK cells. J. Cell Biol. *167*, 531–543.

Bomsel, M., Prydz, K., Parton, R. G., Gruenberg, J., and Simons, K. (1989). Endocytosis in filter-grown Madin-Darby canine kidney cells. J. Cell Biol. *109*, 3243–3258.

Breitfeld, P. P., Harris, J. M., and Mostov, K. E. (1989). Postendocytotic sorting of the ligand for the polymeric immunoglobulin receptor in Madin-Darby canine kidney cells. J. Cell Biol. *109*, 475–486.

Charron, A. J., Bacallao, R. L., and Wandinger-Ness, A. (2000). ADPKD: a human disease altering Golgi function and basolateral exocytosis in renal epithelia. Traffic *1*, 675–686.

Chen, Y. T., Holcomb, C., and Moore, H. P. (1993). Expression and localization of two low molecular weight GTP-binding proteins, Rab8 and Rab10, by epitope tag. Proc. Natl. Acad. Sci. USA *90*, 6508–6512.

Cresawn, K. O., Potter, B. A., Oztan, A., Guerriero, C. J., Ihrke, G., Goldenring, J. R., Apodaca, G., and Weisz, O. A. (2007). Differential involvement of endocytic compartments in the biosynthetic traffic of apical proteins. EMBO J. *26*, 3737–3748.

Daniel, W. W. (1987). Biostatistics: A Foundation for Analysis in the Health Sciences, New York: John Wiley & Sons.

Deretic, D., Huber, L.A., Ransom, N., Mancini, M., Simons, K., and Papermaster, D.S. (1995). rab8 in retinal photoreceptors may participate in rhodopsin transport and in rod outer segment disk morphogenesis. J. Cell Sci. *108* (Pt 1), 215–224.

Drubin, D. G., and Nelson, W. J. (1996). Origins of cell polarity. Cell *84*, 335–344.

Fuller, S. D., and Simons, K. (1986). Transferrin receptor polarity and recycling accuracy in "tight" and "leaky" strains of Madin-Darby canine kidney cells. J. Cell Biol. *103*, 1767–1779.

Futter, C. E., Connolly, C. N., Cutler, D. F., and Hopkins, C. R. (1995). Newly synthesized transferrin receptors can be detected in the endosome before they appear on the cell surface. J. Biol. Chem. *270*, 10999–11003.

Gerges, N. Z., Backos, D. S., and Esteban, J. A. (2004). Local control of AMPA receptor trafficking at the postsynaptic terminal by a small GTPase of the Rab family. J. Biol. Chem. *279*, 43870–43878.

Gravotta, D., Deora, A., Perret, E., Oyanadel, C., Soza, A., Schreiner, R., Gonzalez, A., and Rodriguez-Boulan, E. (2007). AP1B sorts basolateral proteins in recycling and biosynthetic routes of MDCK cells. Proc. Natl. Acad. Sci. USA *104*, 1564–1569.

Grindstaff, K. K., Yeaman, C., Anandasabapathy, N., Hsu, S. C., Rodriguez-Boulan, E., Scheller, R. H., and Nelson, W. J. (1998). Sec6/8 complex is recruited to cell-cell contacts and specifies transport vesicle delivery to the basal-lateral membrane in epithelial cells. Cell *93*, 731–740.

Guo, W., Roth, D., Walch-Solimena, C., and Novick, P. (1999). The exocyst is an effector for Sec4p, targeting secretory vesicles to sites of exocytosis. EMBO J. *18*, 1071–1080.

Gurkan, C., Lapp, H., Alory, C., Su, A. I., Hogenesch, J. B., and Balch, W. E. (2005). Large-scale profiling of Rab GTPase trafficking networks: the membrane. Mol. Biol. Cell *16*, 3847–3864.

Hattula, K., Furuhjelm, J., Arffman, A., and Peranen, J. (2002). A Rab8-specific GDP/GTP exchange factor is involved in actin remodeling and polarized membrane transport. Mol. Biol. Cell *13*, 3268–3280.

Hattula, K., Furuhjelm, J., Tikkanen, J., Tanhuanpaa, K., Laakkonen, P., and Peranen, J. (2006). Characterization of the Rab8-specific membrane traffic route linked to protrusion formation. J. Cell Sci. *119*, 4866–4877.

Hopkins, C. R. (1983). Intracellular routing of transferrin and transferrin receptors in epidermoid carcinoma A431 cells. Cell *35*, 321–330.

Hua, W., Sheff, D., Toomre, D., and Mellman, I. (2006). Vectorial insertion of apical and basolateral membrane proteins in polarized epithelial cells revealed by quantitative 3D live cell imaging. J. Cell Biol. *172*, 1035–1044.

Huber, L. A., de Hoop, M. J., Dupree, P., Zerial, M., Simons, K., and Dotti, C. (1993a). Protein transport to the dendritic plasma membrane of cultured neurons is regulated by rab8p. J. Cell Biol. *123*, 47–55.

Huber, L. A., Pimplikar, S., Parton, R. G., Virta, H., Zerial, M., and Simons, K. (1993b). Rab8, a small GTPase involved in vesicular traffic between the TGN and the basolateral plasma membrane. J. Cell Biol. *123*, 35–45.

Ihrke, G., Martin, G. V., Shanks, M. R., Schrader, M., Schroer, T. A., and Hubbard, A. L. (1998). Apical plasma membrane proteins and endolyn-78 travel through a subapical compartment in polarized WIF-B hepatocytes. J. Cell Biol. *141*, 115–133.

Jordens, I., Marsman, M., Kuijl, C., and Neefjes, J. (2005). Rab proteins, connecting transport and vesicle fusion. Traffic *6*, 1070–1077.

Keller, P., and Simons, K. (1997). Post-Golgi biosynthetic trafficking. J. Cell Sci. *110*, 3001–3009.

Kimura, K., Oka, T., and Nakano, A. (1995). Purification and assay of yeast Sar1p. Methods Enzymol. *257*, 41–49.

Leitinger, B., Hille-Rehfeld, A., and Spiess, M. (1995). Biosynthetic transport of the asialoglycoprotein receptor H1 to the cell surface occurs via endosomes. Proc. Natl. Acad. Sci. USA *92*, 10109–10113.

Matter, K., Whitney, J. A., Miller, E., and Mellman, I. (1993). Common signals control LDL receptor sorting in endosomes and the Golgi of MDCK cells. Cell *74*, 1053–1064.

Moritz, O. L., Tam, B. M., Hurd, L. L., Peranen, J., Deretic, D., and Papermaster, D. S. (2001). Mutant rab8 Impairs docking and fusion of rhodopsin-bearing post-Golgi membranes and causes cell death of transgenic *Xenopus* rods. Mol. Biol. Cell *12*, 2341–2351.

Mostov, K. E., Verges, M., and Altschuler, Y. (2000). Membrane traffic in polarized epithelial cells. Curr. Opin. Cell Biol. *12*, 483–490.

Motulsky, H. J., and Ransnas, L. A. (1987). Fitting curves to data using nonlinear regression: a practical and nonmathematical review. FASEB J. *1*, 365–374.

Murray, R. Z., Wylie, F. G., Khromykh, T., Hume, D. A., and Stow, J. L. (2005). Syntaxin 6 and Vti1b form a novel SNARE complex, which is up-regulated in activated macrophages to facilitate exocytosis of tumor necrosis Factor-alpha. J. Biol. Chem. *280*, 10478–10483.

Nachury, M. V. *et al.* (2007). A core complex of BBS proteins cooperates with the GTPase Rab8 to promote ciliary membrane biogenesis. Cell *129*, 1201–1213.

Nelson, W. J. (2003). Epithelial cell polarity from the outside looking in. News Physiol. Sci. *18*, 143–146.

Oka, T., and Nakano, A. (1994). Inhibition of GTP hydrolysis by Sar1p causes accumulation of vesicles that are a functional intermediate of the ER-to-Golgi transport in yeast. J. Cell Biol. *124*, 425–434.

Paladino, S., Pocard, T., Catino, M. A., and Zurzolo, C. (2006). GPI-anchored proteins are directly targeted to the apical surface in fully polarized MDCK cells. J. Cell Biol. *172*, 1023–1034.

Peranen, J., Auvinen, P., Virta, H., Wepf, R., and Simons, K. (1996). Rab8 promotes polarized membrane transport through reorganization of actin and microtubules in fibroblasts. J. Cell Biol. *135*, 153–167.

Pfeffer, S. R. (1994). Rab GTPases: master regulators of membrane trafficking. Curr. Opin. Cell Biol. *6*, 522–526.

Podbilewicz, B., and Mellman, I. (1990). ATP and cytosol requirements for transferrin recycling in intact and disrupted MDCK cells. EMBO J. *9*, 3477–3487.

Pond, L., and Watts, C. (1997). Characterization of transport of newly assembled, T cell-stimulatory MHC class II-peptide complexes from MHC class II compartments to the cell surface. J. Immunol. *159*, 543–553.

Rogers, K. K., Wilson, P. D., Snyder, R. W., Zhang, X., Guo, W., Burrow, C. R., and Lipschutz, J. H. (2004). The exocyst localizes to the primary cilium in MDCK cells. Biochem. Biophys. Res. Commun. *319*, 138–143.

Roland, J. T., Kenworthy, A. K., Peranen, J., Caplan, S., and Goldenring, J. R. (2007). Myosin Vb interacts with Rab8a on a tubular network containing EHD1 and EHD3. Mol. Biol. Cell *18*, 2828–2837.

Sheff, D. R., Daro, E. A., Hull, M., and Mellman, I. (1999). The receptor recycling pathway contains two distinct populations of early endosomes with different sorting functions. J. Cell Biol. *145*, 123–139.

Sheff, D. R., Kroschewski, R., and Mellman, I. (2002). Actin dependence of polarized receptor recycling in Madin-Darby canine kidney cell endosomes. Mol. Biol. Cell *13*, 262–275.

Simons, K., and Wandinger-Ness, A. (1990). Polarized sorting in epithelia. Cell *62*, 207–210.

Stoorvogel, W., Geuze, H. J., Griffith, J. M., Schwartz, A. L., and Strous, G. J. (1989). Relations between the intracellular pathways of the receptors for transferrin, asialoglycoprotein, and mannose 6-phosphate in human hepatoma cells. J. Cell Biol. *108*, 2137–2148.

Stoorvogel, W., Geuze, H. J., Griffith, J. M., and Strous, G. J. (1988). The pathways of endocytosed transferrin and secretory protein are connected in the trans-Golgi reticulum. J. Cell Biol. *106*, 1821–1829.

Sztul, E., Kaplin, A., Saucan, L., and Palade, G. (1991). Protein traffic between distinct plasma membrane domains: isolation and characterization of vesicular carriers involved in transcytosis. Cell *64*, 81–89.

Thompson, A., Nessler, R., Wisco, D., Anderson, E., Winckler, B., and Sheff, D. (2007). Recycling endosomes of polarized epithelial cells actively sort apical and basolateral cargos into separate subdomains. Mol. Biol. Cell *18*, 2687–2697.

Wandinger-Ness, A., Bennett, M. K., Antony, C., and Simons, K. (1990). Distinct transport vesicles mediate the delivery of plasma membrane proteins to the apical and basolateral domains of MDCK cells. J. Cell Biol. *111*, 987–1000.